2024 19th Iranian Conference on Intelligent Systems (ICIS) 23-24 October, 2024, Sirjan University of Technology, Sirjan, Kerman, Iran

Classification of ASD Based on fMRI Data Using Two Hybrid Learning Approaches

Sara Soltani Gerdefaramarzi
Department of Electrical and Computer Engineering
Isfahan University of Technology
Isfahan, Iran
soltanisara1380@gmail.com

Hamidreza Hakimdavoodi
Department of Electrical and Computer Engineering
Isfahan University of Technology
Isfahan, Iran
hakim@iut.ac.ir

***Abstract*— Autism Spectrum Disorder (ASD) is a neurodevelopmental condition marked by challenges in communication, heightened sensitivity to sensory input, difficulties in adapting to change, and atypical patterns of play. Since traditional methods of diagnosing this disorder rely heavily on behavioral assessments, they are highly prone to errors. Consequently, it is necessary to provide a reliable method for diagnosing this mental disorder by leveraging advanced machine learning techniques. In this paper, two hybrid learning approaches that only use fMRI data have been designed and implemented. The first method is the simultaneous training of a deep autoencoder and a single layer perceptron (SLP) to extract beneficial features and properly tune the model's hyperparameters for classification. The second method combines a support vector machine model with a data augmentation strategy using simultaneous training of a generative adversarial network and a deep autoencoder to prevent model overfitting. It is worth mentioning that in the two proposed methods, the Extra-Trees algorithm is initially used for dimensionality reduction and feature selection. These two methods have been implemented on the entire publicly available dataset released by the Autism Brain Imaging Data Exchange, and both results have been compared. Our study in this paper achieved a maximum accuracy of 70.8%, sensitivity of 67.4%, and specificity of 75.3%. These results indicate that our proposed approaches have performed significantly better than many recent studies in this field.**

Keywords*— *fMRI, ASD, Deep Autoencoder, SLP, Generative Adversarial Network, Extra-Trees, Data Augmentation

I. INTRODUCTION

Autism Spectrum Disorder (ASD) is a complex neurodevelopmental disorder that affects individuals in varying ways, leading to challenges in social interaction, communication, and behavior. The symptoms of ASD can range from mild to severe, which is why it is described as a "spectrum" disorder. Diagnosing ASD traditionally involves behavioral assessments, clinical observations, and developmental history reviews, which can lead to variability in diagnoses. On the other hand, As indicated in (Hirvikoski et al., 2016), premature death is very common among patients with autism. Since there is no guaranteed medication for the complete recovery of individuals with autism, early diagnosis of this condition and subsequent medical interventions can slow the progression of the disease. In this regard, it is necessary to provide a reliable method for diagnosing this mental disorder.

Functional Magnetic Resonance Imaging (fMRI) is a neuroimaging method used to monitor brain activity by tracking variations in blood flow, allowing researchers to visualize which parts of the brain are engaged in particular tasks or cognitive processes (Lindquist, 2008). By analyzing brain activity patterns, fMRI can help identify atypical neural connectivity and functional abnormalities that are often associated with ASD (Hernandez, Rudie, Green, Bookheimer, & Dapretto, 2015). These insights can enhance traditional diagnostic methods by providing objective, neurobiological markers of ASD.

Recently, the diagnosis of ASD using fMRI data, particularly the ABIDE dataset, has garnered significant attention, and numerous studies have been conducted in this area. For instance, (Plitt, Barnes, & Martin, 2015) employed two different subsets of fMRI data. The first subset comprised 59 males with ASD and 59 typically developing (TD) males, matched for age and IQ, while the second subset included an additional 178 individuals (89 ASD and 89 TD) from the ABIDE, also matched for age and IQ. Their final achieved accuracy was 76.67%. In another study, (Sen, Borle, Greiner, & Brown, 2018) implemented a model using structural texture and functional connectivity features extracted from 3-dimensional structural magnetic resonance imaging (MRI) and 4-dimensional resting-state fMRI scans of 1111 total healthy and ASD subjects and gained 64.3% accuracy on ABIDE data. Additionally, the DNN model proposed in (Kong et al., 2019) achieved an accuracy of 90.39% on 182 subjects. The approach proposed in (Nielsen et al., 2013) got 60% accuracy using the combination of functional connectivity between ROIs and demographic information such as age, age-squared, gender, handedness, and site through 964 subjects. Furthermore, (Dvornek, Ventola, Pelphrey, & Duncan, 2017) obtained 68.5% accuracy using the recurrent neural networks with long short-term memory (LSTMs) for classification through the entire ABIDE 1 dataset. Moreover, (Chen et al., 2015) classified 252 subjects with an accuracy of 91% using fMRI data and various machine learning techniques.

In this paper, our goal is to classify patients with autism from typical controls using fMRI data from the whole data repository ABIDE 1. Two hybrid learning methods have been

designed and implemented. The first method combines a deep autoencoder and a SLP to ensure that advantageous features are extracted and the model's parameters are properly tuned. The second method combines a support vector machine model for classification with a data augmentation strategy using simultaneous training of a generative adversarial network and a deep autoencoder to prevent model overfitting. It is worth mentioning that in the two proposed methods, the Extra-Trees algorithm is initially used for dimensionality reduction and feature selection.

It is worth mentioning that only a few recent studies and articles, such as (Heinsfeld, Franco, Craddock, Buchweitz, & Meneguzzi, 2018), (Eslami, Mirjalili, Fong, Laird, & Saeed, 2019), and (Abraham et al., 2017) have targeted the entire dataset. In essence, numerous studies have either analyzed a portion of the dataset or included supplementary information, such as demographic details, within their models. Since we have considered the entire dataset in this paper, we have used the three proposed models in (Heinsfeld et al., 2018), (Eslami et al., 2019), and (Abraham et al., 2017) as baselines to evaluate our models.

The organization of this paper is outlined as follows: The second section offers a concise overview of the dataset employed, the selection of useful features, and finally, the classification using the two proposed hybrid models. In the third section, we discuss the experiments conducted and the results obtained from the models. In the final section, we present the conclusions of the paper.

II. Details Experimental

A. ABIDE Dataset and Preprocessing

This study applied the proposed approaches to the entire ABIDE 1 dataset. This dataset includes fMRI data and demographic information such as gender, age, and IQ of individuals with autism and controls, collected from 17 different centers. The dataset comprises 1112 samples, with 539 samples from individuals with autism and 573 typically developing controls. the preprocessing was performed using the Configurable Pipeline for the Analysis of Connectomes (CPAC) (C. Craddock et al., 2013). Then, data was parcelled into 392 functionally homogeneous ROIs according to the CC400 atlas (R. C. Craddock, James, Holtzheimer III, Hu, & Mayberg, 2012).

To more accurately evaluate our proposed approaches, we compare our results with those published in recent papers, such as studies by (Heinsfeld et al., 2018), (Eslami et al., 2019), and (Abraham et al., 2017) which share the same objective as our study and have been conducted under the same conditions and using the same data. Accordingly, we apply our models to all 871 samples in the dataset, which include 403 ASD subjects and 468 typical control subjects.

B. Feature Selection

In fMRI data, functional connectivity analysis is of great importance, as it assesses the interaction between different brain regions (Van Den Heuvel & Pol, 2010), which can provide distinguishing information to differentiate between individuals with autism and control subjects. For functional connectivity analysis, Pearson's correlation is employed to analyze the relationships between the time series data from various regions (Zhang, Zhang, Chen, Lee, & Shen, 2017). Given two time series u and v of length T, and their respective means $\bar{u}\ and\ \bar{v}$, the Pearson correlation coefficient between these two time series is calculated as follows:

$$\rho_{uv} = \frac{\sum_{t=1}^{T}(u_t - \bar{u})(v_t - \bar{v})}{\sqrt{\sum_{t=1}^{T}(u_t - \bar{u})^2}\sqrt{\sum_{t=1}^{T}(v_t - \bar{v})^2}} \quad (1)$$

Ultimately, for each sample, we will have a correlation matrix with dimensions $n \times n$ where n denotes the count of ROIs, however, given the symmetric nature of this matrix, only the upper triangular part is extracted and used. The remaining values, which amount to $n \times n\ /\ 2$, are considered as the feature vector for each sample. Given that there are 392 regions, the number of features is equivalent to 392 × 392 ⁄ 2 = 76636. However, the number of features is very high and negatively impacts the performance of the models. Therefore, dimensionality reduction is necessary. AS demonstrated in (Liu, Xu, Li, Yu, & Yu, 2020) the Extra-Trees algorithm (Pinto, Pereira, Rasteiro, & Silva, 2018) is used in this context.

The Extra-Trees technique is similar to Random Forests in that it constructs multiple decision trees during training. but it introduces a higher degree of randomness by considering random thresholds for each feature rather than searching for the best possible thresholds (Geurts et al., 2006). According to (Louppe, Wehenkel, Sutera, & Geurts, 2013) Feature importance is calculated based on the average impurity reduction computed from all the trees built. For each tree, each feature's impurity reduction (Gini importance) is computed. Then, the Gini importance for each feature is averaged across all trees to obtain the final feature importance score. The higher the score, the more effective the feature is for classifying the data.

Finally, we selected the 5000 initial features identified by the algorithm as useful and with high scores as the final features for our dataset.

C. First Model: Combination of the Deep Autoencoder and SLP

The proposed model is a combination of a deep autoencoder and a SLP, implemented using the TensorFlow deep learning framework. The model works as follows: first, the deep autoencoder maps the input space with 5000 features to a space with 128 features through a hidden layer. Then, it maps the space with 128 features to a space with 64 features through another hidden layer, and on the other side, a decoder reconstructs the mapped data back to the original space with 5000 features. For training the deep autoencoder, the Mean Squared Error (MSE) loss function is used to calculate the reconstruction error of the data, which is defined as follows:

$$\text{MSE loss} = \frac{1}{N}\sum_{i=1}^{N}(x_i - \hat{x}_i)^2 \quad (2)$$

In this context, N denotes the number of samples, x_i and $\hat{x}_i$ represent the original data and the reconstructed data of the i_{th} sample respectively.

For classifying, a SLP is designed to use the bottleneck layer of the deep autoencoder with a space of 64 features as input. In this output layer, the probability of the data belonging

to the ASD patient class is determined using an activation function denoted as f(x). A threshold of 0.5 is considered, where if the probability is greater than 0.5, the sample belongs to the ASD patient class, and if it is less, it belongs to the control class. This relationship is defined as follows:

$$\hat{y} = \begin{cases} 1 & \text{if } f(x) \geq 0.5 \\ 0 & \text{otherwise} \end{cases} \quad (3)$$

Where $\hat{y}$ represents the predicted class label based on the probability $f(x)$. The binary cross-entropy loss function is used to train SLP. This below function utilizes the true labels of the i_{th} data, denoted as y_i, and the estimated probability of i_{th} data point belonging to the class of individuals with ASD denoted as $f(x_i)$:

$$BCE\ loss = -\frac{1}{N}\sum_{i=1}^{N}\left[y_i \log\left(f(x_i)\right) + (1-y_i)\log\left(1-f(x_i)\right)\right] \quad (4)$$

The key aspect of this model, which leads to its good results, is the simultaneous training of the deep autoencoder and SLP. In each training epoch of this model, the reconstruction error from the decoder (MSE) is summed with the classification error from the SLP (BCE) and used to update the parameters.

According to (Eslami et al., 2019), This simultaneous training ensures that the extracted features are optimal for both the reconstruction of the decoder and for possessing distinguishing information for more accurate data classification. The diagram of the first proposed model is shown in Fig. 1.

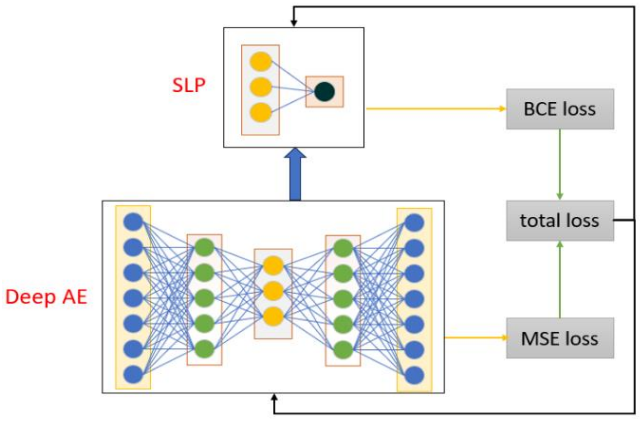

Fig. 1. The structure of the first proposed model consists of a deep autoencoder and a SLP, which are trained simultaneously.

D. *Second Model: Using SVM and Data Augmentation through Generative Adversarial Network and Deep Autoencoder*

In this proposed method, according to (Liu et al., 2020) the SVM model is used for classifying samples, and the model Hyperparameters such as kernel type, regularization constant (C), and kernel coefficient (γ) are first tuned using the grid search method.

When working with machine learning or deep learning models, it is essential to have a sufficient amount of data to avoid overfitting (Ying, 2019). Nevertheless, large training datasets are not always accessible, and acquiring additional data can be expensive, particularly in domains such as medical imaging. Therefore, data augmentation techniques using artificial intelligence can be implemented. In this regard, a combination of GAN architecture (Goodfellow et al., 2014) and deep autoencoder was used to generate synthetic data.

Generative Adversarial Networks (GANs) represent a category of machine learning models that involve two neural networks—the generator and the discriminator—engaged in a zero-sum competition. In this framework, the generator seeks to produce increasingly convincing fake data to mislead the discriminator, whereas the discriminator works to enhance its ability to differentiate between genuine and counterfeit data. The generator's objective is to reduce the likelihood that the discriminator correctly classifies its synthetic outputs. Conversely, the discriminator aims to maximize its accuracy in detecting real versus fake data (Sajeeda & Hossain, 2022).

In this implementation, data augmentation is achieved using a combination of a deep autoencoder and a GAN structure, which consists of an encoder, a decoder, and a discriminator. It is worth mentioning that in this model, the decoder functions as the generator within the GAN structure. Initially, in the encoder with two hidden layers, the input data, which are the training data, are mapped from a space with 5000 features to a space with 512 features in the first layer, then to a space with 256 features in the next layer, and finally to a space with 128 features in the output layer. On the other hand, the decoder acts like a generator that aims to generate new samples by reconstructing the original input space from the latent space. Therefore, it needs to transform the data from a space with 128 features back to a space with 5000 features. As (Sajeeda & Hossain, 2022) mentioned, the discriminator is also a neural network model that distinguishes between fake and real data. This model returns an output representing the probability that indicates the data is real or fake. The closer this probability is to one, the more real the data is; the closer it is to zero, the more likely the data is fake.

The discriminator is first trained using binary cross-entropy loss function in the model training phase. The loss function for the discriminator is defined as follows:

$$\mathcal{L}_D = -\mathbb{E}_{x\sim p_{\text{data}}}[\log D(x)] - \mathbb{E}_{\hat{x}\sim p_{\text{fake}}}\left[\log\left(1-D(\hat{x})\right)\right] \quad (5)$$

Where x represents the real samples and $\hat{x}$ represents the samples generated by the generator in the original feature space with 5000 features. Additionally, $D(x)$ and $D(\hat{x})$ represent the discriminator's output when fed with real data and generated data, respectively. The logic behind this equation is as follows: given that the discriminator's goal is to

improve its ability to distinguish between real and fake data, the closer D(x) is to one (indicating the probability that the data is real), the better the discriminator is performing. This is because real data x is being correctly identified with high probability. In this case, the logarithm of this probability increases, and since this value needs to be minimized in the loss calculation, it becomes negative. On the other hand, the better the discriminator performs in identifying fake data with a probability close to zero, the more effective it is. Therefore, the smaller $D(\hat{x})$ is, the larger 1 - $D(\hat{x})$ is, and consequently, the logarithm of this value increases. This value needs to be minimized in the loss function, so it becomes negative. Finally, these values are summed to improve the discriminator's performance in handling both real and fake data.

In the second step, it is necessary to train the encoder and decoder together. The loss function for the generator or decoder is defined as follows:

$$\mathcal{L}_{\mathrm{G}} = -\mathbb{E}_{\hat{\mathrm{x}}\sim \mathrm{p}_{\mathrm{fake}}}[\log \mathrm{D}(\hat{\mathrm{x}})] \quad (6)$$

We know that the goal of the generator is to produce data in such a way that the discriminator cannot distinguish it from real data. Therefore, we want the discriminator to assign a probability close to one when encountering fake or reconstructed data, essentially recognizing them as real data. Therefore, the higher the probability, the greater the logarithm value. To minimize the error, this value needs to be negative. On the other hand, the reconstruction error of the decoder, which determines the difference between the real data and the reconstructed data, is calculated using the mean squared error (MSE) and is defined as follows:

$$\mathcal{L}_{rec} = \mathbb{E}_{x\sim p_{\mathrm{data}}}[\| x - \hat{x} \|^2] \quad (7)$$

Finally, the two error values calculated above ($\mathcal{L}_G$, $\mathcal{L}_{rec}$) are summed together to use the combined loss for updating the parameters of the encoder and decoder, thereby training both models. So, the deep autoencoder and the GAN model need to be trained simultaneously.

Simultaneous training of the deep autoencoder and the GAN architecture allows the generator to produce more realistic data. This is because, in addition to considering the loss resulting from the decoder as a generator of synthetic data within the GAN structure (where the generator strives to produce more realistic data by leveraging the discriminator), the reconstruction error of mapping the data in the latent space back to the original space is also taken into account (while the decoder aims to closely reconstruct the data to resemble the original data). Then, efforts are made to minimize this error as well.

After these three models, the encoder, the decoder (generator), and the discriminator, have been trained for 100 epochs and the loss has been minimized, samples are generated through the decoder in the space with 128 features. These samples are then reconstructed and transformed back to the original space with 5000 features by decoder (generator), serving as synthetic data. In Fig. 2, a schematic of the GAN structure alongside the deep autoencoder, which is used for data augmentation, is shown.

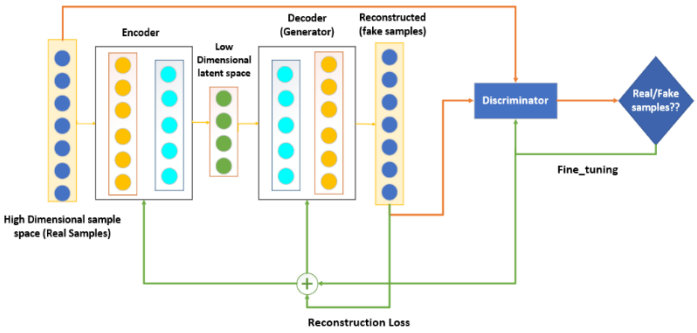

Fig. 2. A data augmentation structure consisting of a deep autoencoder and a GAN architecture, where these two models are trained simultaneously.

With data augmentation, one synthetic sample is generated for each training sample, resulting in the doubling of the training dataset size.

III. Results and Discussion

Given that the NVIDIA Tesla T4 is a versatile and powerful GPU, it is well-suited for modern AI and machine learning workloads, offering a balance of performance, efficiency, and scalability, the models were executed using a T4 GPU (Alqahtani, 2024).

In this section, we evaluate the performance of the two proposed hybrid models by applying k-fold cross-validation on the entire dataset. Given that the models are applied to the whole dataset containing sufficient samples, we use k=10 for k-fold cross-validation by randomly shuffling and splitting the dataset into 10 folds. This ensures enough samples for testing (87 samples) and training (784 samples) in each iteration. To evaluate the models, we use the metrics of accuracy, sensitivity, and specificity, similar to other studies such as (Heinsfeld et al., 2018), (Eslami et al., 2019), and (Abraham et al., 2017). Accuracy indicates the percentage of correctly classified samples by the model. Sensitivity refers to the model's ability to accurately identify actual positive cases (individuals with autism). Specificity, in contrast, measures the proportion of true negative cases (healthy controls) that the model successfully detects.

To evaluate our implemented models, we considered baselines such as Support Vector Machine and Random Forest, as well as models proposed by other papers on the same dataset with similar objectives, such as (Heinsfeld et al., 2018), (Eslami et al., 2019), and (Abraham et al., 2017). The SVM and Random Forest models were run on the preprocessed dataset (the preprocessing for these baselines and our proposed model is the same as described). However, since the feature dimensions were not reduced by the Extra-Trees method, these two baselines were executed on the dataset with the original number of features. The best values for the hyperparameters of these two models (kernel type, regularization constant (C), and kernel coefficient (γ) for SVM and the number of trees, the maximum depth of trees in the Random Forest) were determined using the grid search method.

A. *Experiments Using the CC400 Atlas*

In this section, using the 10-fold cross-validation method, we applied both proposed models along with the provided

baselines on all 871 samples of the dataset using the CC400 atlas. Table I presents a comparison of the evaluation metrics achieved by the first proposed model, the second proposed model (with and without data augmentation), and the Random Forest and Support Vector Machine models (without feature dimension reduction).

TABLE I. CLASSIFICATION RESULTS USING 10-FOLD CROSS-VALIDATION BASED ON CC400 ATLAS

Method	Evaluation Metrics		
	Accuracy	***Sensitivity***	***Specificity***
Second Model	**70.8**	65.6	**75.3**
Second Model (no aug)	68.1	62.2	73.2
First Model	70.2	**67.4**	72.7
SVM	66.3	65	71.4
Random Forest	60.6	59.8	70.7

As the results in Table I indicate, our proposed models performed better than the other baselines with 70.2% and 70.8% accuracy, respectively. Additionally, the data augmentation in the second model increased the accuracy by 2% to 3%.

B. Experiments on Other Atlas

the choice of atlas significantly impacts the performance of the proposed models. In this regard, the performance of both proposed approaches is evaluated using the CC200 (R. C. Craddock et al., 2012) atlas, which divides the brain volume into 200 ROIs, and the results are compared. Similar to the CC400 atlas, the Pearson correlation between different regions is calculated and considered as features. Then, the 5000 best features obtained through the Extra-Trees algorithm are selected as the essential features needed. In fact, out of the 19,900 features obtained from the CC200 atlas only 5000 final features are selected. The results of applying both proposed models along with the considered baselines using 10-fold cross-validation on all dataset samples with the use of the CC200 atlas are shown in Table II.

TABLE II. CLASSIFICATION RESULTS USING 10-FOLD CROSS-VALIDATION BASED ON CC200 ATLAS

Method	Evaluation Metrics		
	Accuracy	***Sensitivity***	***Specificity***
Second Model	70	61.4	71.1
Second Model (no aug)	67.9	61.6	73.4
First Model	70.3	66.1	73.6
SVM	65	68	62
Random Forest	63	69	58

As evident from the results above, The first model performed slightly better on CC200, but the second model showed a more significant improvement on CC400, and ultimately, the best result was achieved by applying the second model on CC400, because the connectivity among the ROIs in CC400 provides more distinguishing information than in CC200 and the best brain atlas is CC400 as also shown in (Yang, Islam, & Khaled, 2019).

C. Recent Papers Considered as Baselines

In Table III, the results of the three proposed models presented by (Heinsfeld et al., 2018), (Eslami et al., 2019), and (Abraham et al., 2017) studies which have been considered as baselines for our models are shown.

TABLE III. CLASSIFICATION RESULTS REPORTED BY RECENT PAPERS

Method	Evaluation Metrics		
	Accuracy	***Sensitivity***	***Specificity***
Proposed Model in (Abraham et al., 2017)	66.9	53.2	78.3
Proposed Model in (Heinsfeld et al., 2018)	70	74	63
Proposed Model in (Eslami et al., 2019)	70.3	68.3	72.2

By comparing the results of our two proposed models with the results from recent articles, we observe that the first model outperformed two of these studies with an accuracy improvement of 0.3% and 3.4%. In contrast, the second model achieved the best result, which surpassed the results of all three papers with an accuracy increase of 0.5% to 4%.

IV. CONCLUSION

The main objective of this study was to distinguish individuals with autism from typically developing controls using fMRI data. To achieve this, we used the entire ABIDE 1 dataset. Functional connectivities were used as features due to their valuable information, but the Extra-Trees algorithm was applied to reduce dimensionality and select 5000 useful features. Two combined models were then proposed. The first model involves implementing a deep autoencoder for extracting useful features in conjunction with a SLP for classifying, which is trained simultaneously. The second model employs a Support Vector Machine for classification and uses simultaneous training of a GAN architecture and a deep autoencoder for data augmentation. In conclusion, we implemented these two models with 10-fold cross-validation on the dataset, leading to an improvement in classification accuracy compared to the findings of some recent studies that worked on the entire ABIDE 1 dataset with the same objective. Specifically, the first model achieved an accuracy of 70.3%, while the second model reached an accuracy of 70.8%.

REFERENCES

[1] Abraham, A., Milham, M. P., Di Martino, A., Craddock, R. C., Samaras, D., Thirion, B., & Varoquaux, G. (2017). Deriving reproducible biomarkers from multi-site resting-state data: An Autism-based example. NeuroImage, 147, 736-745.

[2] Alqahtani, O. M. (2024). Efficient Deep Learning for Plant Disease Classification in Resource Constrained Environment. University of Georgia,

[3] Chen, C. P., Keown, C. L., Jahedi, A., Nair, A., Pflieger, M. E., Bailey, B. A., & Müller, R.-A. (2015). Diagnostic classification of intrinsic functional connectivity highlights somatosensory, default mode, and visual regions in autism. NeuroImage: Clinical, 8, 238-245.

[4] Craddock, C., Benhajali, Y., Chu, C., Chouinard, F., Evans, A., Jakab, A., . . . Milham, M. (2013). The neuro bureau preprocessing initiative: open sharing of preprocessed neuroimaging data and derivatives. Frontiers in neuroinformatics, 7(27), 5.

[5] Craddock, R. C., James, G. A., Holtzheimer III, P. E., Hu, X. P., & Mayberg, H. S. (2012). A whole brain fMRI atlas generated via spatially constrained spectral clustering. Human brain mapping, 33(8), 1914-1928.

[6] Dvornek, N. C., Ventola, P., Pelphrey, K. A., & Duncan, J. S. (2017). Identifying autism from resting-state fMRI using long short-term memory networks. Paper presented at the Machine Learning in Medical Imaging: 8th International Workshop, MLMI 2017, Held in Conjunction with MICCAI 2017, Quebec City, QC, Canada, September 10, 2017, Proceedings 8.

[7] Eslami, T., Mirjalili, V., Fong, A., Laird, A. R., & Saeed, F. (2019). ASD-DiagNet: a hybrid learning approach for detection of autism spectrum disorder using fMRI data. Frontiers in neuroinformatics, 13, 70.

[8] Goodfellow, I., Pouget-Abadie, J., Mirza, M., Xu, B., Warde-Farley, D., Ozair, S., . . . Bengio, Y. (2014). Generative adversarial nets. Advances in neural information processing systems, 27.

[9] Heinsfeld, A. S., Franco, A. R., Craddock, R. C., Buchweitz, A., & Meneguzzi, F. (2018). Identification of autism spectrum disorder using deep learning and the ABIDE dataset. NeuroImage: Clinical, 17, 16-23.

[10] Hernandez, L. M., Rudie, J. D., Green, S. A., Bookheimer, S., & Dapretto, M. (2015). Neural signatures of autism spectrum disorders: insights into brain network dynamics. Neuropsychopharmacology, 40(1), 171-189.

[11] Hirvikoski, T., Mittendorfer-Rutz, E., Boman, M., Larsson, H., Lichtenstein, P., & Bölte, S. (2016). Premature mortality in autism spectrum disorder. The British Journal of Psychiatry, 208(3), 232-238.

[12] Kong, Y., Gao, J., Xu, Y., Pan, Y., Wang, J., & Liu, J. (2019). Classification of autism spectrum disorder by combining brain connectivity and deep neural network classifier. Neurocomputing, 324, 63-68.

[13] Lindquist, M. A. (2008). The statistical analysis of fMRI data.

[14] Liu, Y., Xu, L., Li, J., Yu, J., & Yu, X. (2020). Attentional connectivity-based prediction of autism using heterogeneous rs-fMRI data from CC200 atlas. Experimental neurobiology, 29(1), 27.

[15] Louppe, G., Wehenkel, L., Sutera, A., & Geurts, P. (2013). Understanding variable importances in forests of randomized trees. Advances in neural information processing systems, 26.

[16] Nielsen, J. A., Zielinski, B. A., Fletcher, P. T., Alexander, A. L., Lange, N., Bigler, E. D., . . . Anderson, J. S. (2013). Multisite functional connectivity MRI classification of autism: ABIDE results. Frontiers in human neuroscience, 7, 599.

[17] Pinto, A., Pereira, S., Rasteiro, D., & Silva, C. A. (2018). Hierarchical brain tumour segmentation using extremely randomized trees. Pattern Recognition, 82, 105-117.

[18] Plitt, M., Barnes, K. A., & Martin, A. (2015). Functional connectivity classification of autism identifies highly predictive brain features but falls short of biomarker standards. NeuroImage: Clinical, 7, 359-366.

[19] Sajeeda, A., & Hossain, B. M. (2022). Exploring generative adversarial networks and adversarial training. International Journal of Cognitive Computing in Engineering, 3, 78-89.

[20] Sen, B., Borle, N. C., Greiner, R., & Brown, M. R. (2018). A general prediction model for the detection of ADHD and Autism using structural and functional MRI. PloS one, 13(4), e0194856.

[21] Van Den Heuvel, M. P., & Pol, H. E. H. (2010). Exploring the brain network: a review on resting-state fMRI functional connectivity. European neuropsychopharmacology, 20(8), 519-534.

[22] Yang, X., Islam, M. S., & Khaled, A. A. (2019). Functional connectivity magnetic resonance imaging classification of autism spectrum disorder using the multisite ABIDE dataset. Paper presented at the 2019 IEEE EMBS international conference on biomedical & health informatics (BHI).

[23] Ying, X. (2019). An overview of overfitting and its solutions. Paper presented at the Journal of physics: Conference series.

[24] Zhang, Y., Zhang, H., Chen, X., Lee, S.-W., & Shen, D. (2017). Hybrid high-order functional connectivity networks using resting-state functional MRI for mild cognitive impairment diagnosis. Scientific reports, 7(1), 6530.